

Mechanistic and reaction engineering aspects of nitrile hydrogenation

Peter Schärringer, Thomas E. Müller, Johannes A. Lercher

Department Chemie, Lehrstuhl II für Technische Chemie, Technische Universität München, Lichtenbergstr. 4, 85747 Garching, Germany, Tel. +49 89 28912827, Fax +49 89 28913544, E-Mail: thomas.mueller@tum.de

1. Abstract

Liquid phase hydrogenation of nitriles is an important method for the production of primary amines, which find a variety of applications as intermediates in chemical and pharmaceutical industry. Raney-Co or supported Cobalt catalysts are frequently used due to the relatively high selectivity to primary amines. However, selectivities in excess of 95% can only be achieved, when ammonia is used as solvent. Thereby, thermodynamic control of the reaction is achieved as condensation reactions, where ammonia is released, are suppressed. However, liquid ammonia is difficult to handle and it is highly interesting to avoid, or at least to minimise, the addition of ammonia. This requires kinetic control of the reaction by optimizing catalyst properties and process conditions.

Keywords: Multi-phase reaction, Trickle-bed reactor, Hydrogenation, Cobalt catalyst, Nitrile

2. Introduction

Primary amines are often used as feedstock in the production of, e.g., of fibres for textiles and surface-active compounds. One important industrial process for their manufacture is the hydrogenation of the corresponding nitriles over transition metal catalysts,¹ which is usually accompanied by the formation of secondary and tertiary amines as undesired by-products.² However, in certain applications even very small quantities of the by-products result in poor quality of the final product.^{3,4} Understanding the development of by-products from a mechanistic point of view is considered as an essential prerequisite for further optimization of catalysts and consequently higher selectivity. Already in 1923 it was suggested that the side reactions proceed via reactive aldimine intermediates² and ever since numerous mechanistic discussions were based on von Braun's proposal.⁵⁻⁷ As direct observation of the aldimine had not been reported⁵ other possible surface intermediates, such as carbenes and nitrenes, were included in the discussion.⁸⁻¹⁰

A widely used class of catalysts are skeletal Raney catalysts based on Co or Ni.¹¹ Compared to other transition metals (e.g. Ni and Ru) Co is known to exhibit the highest selectivity to primary amines but generally provides relatively low activity.¹² A present study in our group aims at establishing structure-selectivity correlations for Raney-Co¹³⁻¹⁵ with the aim to generate information on how to enhance the selectivity on highly active hydrogenation catalysts.

For studying the sorption of hydrogen containing molecules on metal surfaces Inelastic Neutron Scattering (INS) has proven to be a useful tool.¹⁶⁻¹⁸ As the cross-section of hydrogen is 10-100 times larger than that of all other elements¹⁹, INS is particularly sensitive for vibrations involving hydrogen atoms during the sorption of hydrogen and nitriles on Raney catalysts.^{13, 20-22}

In this work, special emphasis was given to the identification of the surface intermediates formed during the hydrogenation of nitriles over a Raney-Co catalyst to unravel the elementary steps on the metal surface. The co-adsorption of acetonitrile- d_3 (CD_3CN) and hydrogen on Raney-Co was investigated as a model reaction. The choice of this model is based on the idea that during the hydrogenation of the CN triple bond the C-H vibrations of the resulting intermediates and the product will be much more pronounced in the INS spectrum compared to the C-D vibrations of the reactant. Thus, a better differentiation between the reactant and surface intermediates will be obtained.

3. Experimental

3.1. Materials

Raney-Co 2700 catalyst (Grace Davison division of W.R. Grace and Co.) was received as an aqueous suspension. The chemical composition was: 1.85 wt% Al; 97.51 wt% Co; 0.3 wt% Fe and 0.34 wt% Ni. It was washed with de-ionized water under nitrogen atmosphere until the pH of the washing water was ~ 7 . Due to its sensitivity to oxygen, the catalyst was stored and handled under inert atmospheres throughout all further steps. The remaining water was removed by drying in partial vacuum ($p < 1$ kPa) for 30 h at 323 K. CD_3CN (Deutero GmbH), CH_3CN (Fluka) and acetaldehyde (Riedel-de Haën) with a purity of 99.5% each were used as received. Deuterium labelled *n*-ethylamine ($CD_3CH_2NH_2$) was obtained by hydrogenation of CD_3CN over Raney-Co 2700.

3.2. Catalyst characterization

H_2 -chemisorption and N_2 -physisorption (BET) were measured on a Sorptomatic 1990 instrument (ThermoFinnigan). For both measurements the catalyst sample (~ 1 g) was outgassed for 6 h at 473 K ($p < 1$ mPa). The BET measurement was conducted at 77 K. H_2 -chemisorption was carried out at 308 K with an equilibrating time of 2 – 180 min for each pressure step. Equilibration was continued until the pressure deviation was < 0.27 mbar within of a 2-min period. Isotherms were measured twice on the sample. Between the two measurements, the sample was evacuated to 10^{-3} mbar for 1h. The second isotherm (physisorbed H_2) was subtracted from the first isotherm

(chemisorbed and physisorbed H_2). The amount of hydrogen adsorbed was determined by extrapolating the linear part of the difference isotherm ($p > 6.5$ kPa) to zero pressure. The number of accessible metal atoms was calculated assuming that one hydrogen atom was adsorbed per cobalt atom. By assuming a transversal section of 6.5 \AA^2 per cobalt atom, the metal surface area was determined from the amount of chemisorbed hydrogen.

The adsorption of gaseous CD_3CN on Raney-Co was investigated on a Setaram TG-DSC 111 thermoanalyzer. Before the measurement the catalyst sample (~ 24 mg) was outgassed for 6 h at 473 K ($p < 0.1$ mPa). Adsorption of CD_3CN was carried out at 308 K using pressure pulses of 0.02 – 2.5 mbar up to ~ 11 mbar. The weight increase and the corresponding heat flux were recorded for each pulse.

The hydrogenation of CD_3CN was conducted in a stirred tank reactor (160 cm^3 ; Parr Instrument Comp.) at constant hydrogen pressure by re-supplying hydrogen consumed during the reaction. Raney-Co catalyst (1 g) was suspended in the reaction mixture composed of CD_3CN (40 cm^3) and hexane (40 cm^3) under inert atmosphere. Hexane was used both as solvent and as internal standard for GC chromatography. The suspension was filled into the autoclave under a flow of nitrogen. After closing, the reactor was pressurized and depressurized five times with nitrogen to remove oxygen. The reaction mixture was heated to the reaction temperature (383 K). The reaction was started by rapidly pressurizing the reactor with hydrogen to 45 bar and subsequently starting the stirrer (1500 rpm). Samples for off-line NMR and GC analysis were periodically withdrawn through a dip-tube with a filter for solids. GC analysis was carried out on an HP Gas Chromatograph 5890 equipped with a cross linked 5% diphenyl-95% dimethylpolysiloxane column (Rtx-5 Amine, 30 m, Restek GmbH). 1H NMR and 2H NMR measurements were carried out on a Bruker DPX-400 (400 MHz) instrument with CD_3Cl as solvent containing 1 vol.-% trimethylsilane as standard. The selectivity was calculated as the ratio of the product yield to the amount of CD_3CN converted.

Inelastic neutron scattering measurements (INS) were performed on 3-axis spectrometer IN1 at the Institut Laue-Langevin (Grenoble, France) using a Beryllium filter-analyser (BeF) and a Cu (220) monochromator, which allows INS spectra to be recorded in the energy transfer range $213 - 2500 \text{ cm}^{-1}$ using neutrons from the hot source. IN1-BeF is optimized for the phonon density-of-states measurements, studies of molecular dynamics and atomic bonding in hydrogen-containing matter, materials and compounds.²³

The samples of the pre-dried Raney-Co catalyst (each ~ 45 g) were transferred to cylindrical aluminum containers (height: 7.5 cm; diameter: 2.3 cm) under inert atmosphere. Subsequently, the samples were activated in vacuum ($p < 1$ mPa) at 473 K for 6 h. The amount of CD_3CN added in liquid form was calculated with respect to two boundary conditions. To assure that only CD_3CN or reaction intermediates, which are adsorbed on the catalyst, contribute to the signal, excess CD_3CN in the sample container has to be avoided. On the other hand, to obtain sufficient signal intensity it is necessary use the maximum possible amount of CD_3CN in the INS cell. Thus, to estimate the maximum amount of CD_3CN , which can be adsorbed on the surface of the Raney-Co catalyst the adsorption of CD_3CN was followed by thermogravimetry and calorimetry. The maximum uptake was ~ 0.30 mole-

cules/ $\text{Co}_{\text{Surface}}$. For adsorption of ethylamine- d_3 ($\text{CD}_3\text{CH}_2\text{NH}_2$) the same molar loading as for CD_3CN was used.

Four sample containers filled with CD_3CN were equilibrated with hydrogen to obtain a ratio of 0.5, 1.0, 1.5 and 2.0 $\text{mol}_{\text{H}_2}/\text{mol}_{\text{CD}_3\text{CN}}$. The amount of CD_3CN and of hydrogen added to the samples is summarized in Table 1. After sealing, the aluminum containers were heated to 333 K for 10 h to ensure even distribution of the adsorbate and to start the reaction of CD_3CN with hydrogen.

For the INS experiments, the sample containers were inserted in the cryostat and cooled to 10 K. The spectra were recorded in the energy range 213 – 2070 cm^{-1} with a resolution of 16 cm^{-1} , 8 cm^{-1} and 32 cm^{-1} at energy transfers between 213 – 760 cm^{-1} , 760 – 1745 cm^{-1} and 1745 – 2070 cm^{-1} , respectively. In order to test the reproducibility of the sample preparation procedure and INS measurements, the same experiments were carried out in two different measurement cycles. The results from the two cycles showed good agreement.

Tab. 1: Amounts of catalyst, CD_3CN , $\text{CD}_3\text{CH}_2\text{NH}_2$ and hydrogen filled into the sample cells for INS measurement.

Sample	Amount of catalyst [g]	Amount of CD_3CN / $\text{CD}_3\text{CH}_2\text{NH}_2$ [mmol]	Amount of hydrogen [mmol]
Raney-Co	45.42	-	-
Raney-Co + H_2	38.94	-	10.36
Raney-Co + CD_3CN	44.98	8.80	-
Raney-Co + CD_3CN + 0.5 eq. H_2	45.23	8.85	4.43
Raney-Co + CD_3CN + 1.5 eq. H_2	45.27	8.86	13.29
Raney-Co + CD_3CN + 2.0 eq. H_2	44.70	8.75	17.50
Raney-Co + $\text{CD}_3\text{CH}_2\text{NH}_2$	45.80	8.96	-

The vibrational frequencies of the characteristic groups were calculated after optimizing the structure of the different molecules with respect to the total energy using density functional theory (DFT) as implemented in GAUSSIAN 03.²⁴ The B3LYP hybrid functional and a 6-31G** basis set were applied. The displacement vectors calculated for each vibrational mode were used to derive the INS-spectra with the program a-CLIMAX^{25, 26} and the vibrational modes were visualized and assigned with Molview 3.0.

4. Results and discussion

4.1. Adsorption of H_2 and CD_3CN on Raney-Co

Though Raney-Co is almost 100% pure cobalt under the conditions applied both reversibly (physisorbed) and irreversibly bound (chemisorbed) hydrogen were observed in H_2 chemisorption measurement is shown (Fig. 1). Assuming a stoichiometry of 2 H atoms per Co atom for physisorption and 1 H atom per Co atom for chemisorption the overall number of surface metal atoms adsorbing H_2 was determined to be 0.46 $\text{mmol}\cdot\text{g}_{\text{Cat}}^{-1}$, the number of metal atoms physisorbing and chemisorbing H_2 was 0.10 $\text{mmol}\cdot\text{g}_{\text{Cat}}^{-1}$ and 0.36 $\text{mmol}\cdot\text{g}_{\text{Cat}}^{-1}$, respectively. Hence, physisorption took place on

approximately 22% of the overall number of surface metal atoms. Assuming a transversal section of 6.5 \AA^2 for Co, the metal surface area was calculated to $18.7 \text{ m}^2 \cdot \text{g}_{\text{Cat}}^{-1}$ based on the overall number of accessible metal atoms. The BET area obtained by N_2 physisorption was $29.1 \text{ m}^2 \cdot \text{g}_{\text{Cat}}^{-1}$.

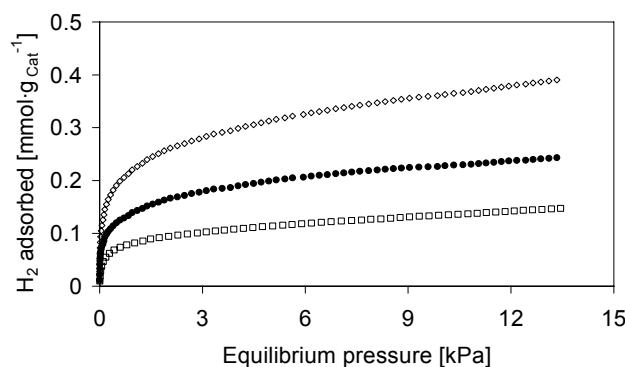


Fig. 1: H_2 chemisorption data for Raney-Co ($T = 308 \text{ K}$). (\diamond) after outgassing for 6 h at $T = 473 \text{ K}$, (\square) after subsequent evacuation at $T = 308 \text{ K}$ ($p < 1 \text{ mPa}$ for 1 h), (\bullet) difference of (\diamond) and (\square). The amount adsorbed is obtained by extrapolating the linear part ($p = 6 \text{ kPa} - 13 \text{ kPa}$) of the respective curve to zero pressure.

Insight into the relative number and strength of different sorption sites was obtained by adsorption of CD_3CN . The sorption isotherm and the heat of adsorption as a function of the coverage (molecules of CD_3CN per surface atom of cobalt chemisorbing hydrogen [$\text{molecule}/\text{Co}_{\text{Surface}}$]) are shown in Fig. 2 and Fig. 3, respectively. The coverage significantly increased at low pressures. The value was quantified by the fitting procedure described below. The differential heat of adsorption was high ($200 - 215 \text{ kJ} \cdot \text{mol}^{-1}$) at low uptake ($< 0.08 \text{ molecules}/\text{Co}_{\text{Surface}}$) and showed a sharp decrease reaching an almost constant value of $57 - 65 \text{ kJ} \cdot \text{mol}^{-1}$ at higher coverage. The remarkably high heat of adsorption at low coverage can be attributed to the adsorption of CD_3CN on sites that strongly interact with the sorbate. Possibly, defect sites were present in small concentrations. At higher coverage sites, which exhibit weaker interaction with the sorbate resulted in lower heat of adsorption.

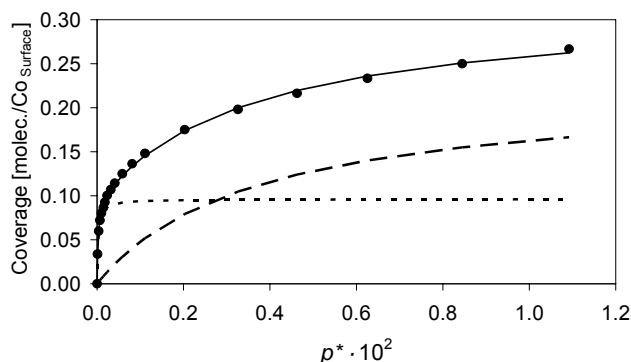


Fig. 2: Sorption isotherm CD_3CN on Raney-Co at 308 K . (\bullet) Experimental data and fitted curves with (----) K_1 and q_1^{sat} , (-.-) K_2 and q_2^{sat} , (—) sum of both fitted curves. p^* is the partial pressure of CD_3CN normalized to standard conditions (i.e. $p^* = p/p^0$).

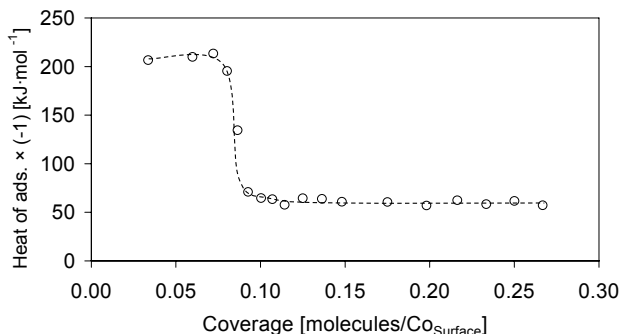


Fig. 3: Differential heat of adsorption of CD_3CN on Raney-Co from calorimetry at 308 K.

The isotherm in Fig. 2 was described by a dual-site Langmuir model in order to verify the assumption of two different adsorption sites. Therefore, the data was fitted with the following equation:²⁷

$$q = \sum_{j=1}^n q_j^{\text{sat}} \frac{K_j \cdot p^*}{1 + K_j \cdot p^*} \quad \text{Equ. 1}$$

in which K_j is the thermodynamic equilibrium constant for the sorption process on the site j , q_j^{sat} denotes the maximum sorption capacity on site j (molecules/metal atom) and p^* is the partial pressure of CD_3CN normalized to standard conditions ($p^* = p/p^0$). The contributions of the individual sorption processes are included in Table 2. The equilibrium constant of the sorption process 1 indicates a much stronger heat of adoption than for sorption process 2. In agreement with the sharp decrease in the heat of adsorption measured at a coverage of the sites involved in the sorption process 1 is also $q_1^{\text{sat}} \sim 0.1$ molec/Co. Note that a fraction of $\sim 30\%$ of the overall number of sites is composed of strong sites (Sorption process 1). The sum of the saturation values of the two steps indicates that the overall saturation value approached ~ 0.3 molecules/ $\text{Co}_{\text{Surface}}$.

Tab. 2: Dual site Langmuir model for fitting the experimental sorption isotherm of CD_3CN on Raney-Co.

Sorption process	q_j^{sat} [molec./ $\text{Co}_{\text{Surface}}$]	K_j	$\Delta H_{\text{ads}} \times (-1)$ [$\text{kJ} \cdot \text{mol}^{-1}$]
1	9.62×10^{-2}	3.94×10^4	200 – 215
2	22.23×10^{-2}	2.73×10^2	57 – 65

4.2. H/D exchange and selectivity in the hydrogenation of CD_3CN

In INS, motions involving H atoms exhibit high signal intensity, thus the use of D exchanged acetonitrile and gaseous H_2 will allow identify the H atoms added in the hydrogenation reaction especially in partially hydrogenated species on the catalyst surface. A low background was achieved by using a fully deuterated test molecule (CD_3CN). However, this approach is appropriate only, if exchange between H atoms reacting with the nitrile group and D atoms from the methyl group can be excluded.

Therefore, hydrogenation of CD_3CN over Raney-Co was carried out in the liquid phase and analyzed off-line by ^1H and ^2H NMR spectroscopy to investigate the intramolecular distribution of H and D atoms. The focus here will be on examination of the H/D exchange with respect to the applicability in the INS experiments. A detailed discussion of the underlying mechanism will be presented in a parallel study.

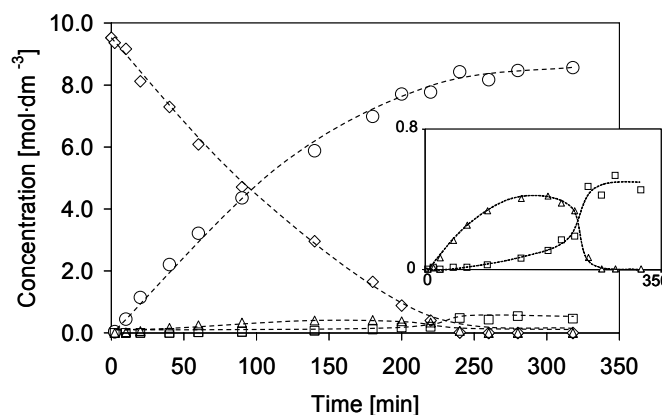


Fig. 4: Concentration profile for the hydrogenation of CD_3CN over Raney-Co at 383 K, $p = 45$ bar and $c_0(\text{CD}_3\text{CN}) = 9.52 \text{ mol}\cdot\text{dm}^{-3}$. (◇) CD_3CN , (○) Ethylamine, (△) *N*-ethylidene-ethylamine, (◻) Di-ethylamine.

A concentration profile of the reaction derived from GC analysis is shown in Fig. 4. The main product of the hydrogenation reaction was ethylamine- d_3 , which was formed with a selectivity of $\sim 90\%$. From the beginning of the reaction ethylamine and the intermediate *N*-ethylidene-ethylamine were found in the reaction mixture, which suggests that both are primary products. Only after most of CD_3CN ($\sim 90\%$) had been converted, the intermediate was further hydrogenated to the secondary product di-ethylamine. The selectivity obtained in the experiment was considered sufficient to prepare $\text{CD}_3\text{CH}_2\text{NH}_2$, which was used as a reference substance for INS measurements, by this procedure.

^1H NMR and ^2H NMR spectra of the final product mixture are shown in Fig. 5. The main product was $\text{CD}_3\text{CH}_2\text{NH}_2$ (peaks at 1.02 and 2.74 ppm in ^1H NMR and at 1.10 in ^2H NMR). Peaks with low intensity at 2.63 and at 2.74 ppm in ^2H NMR correspond to $(\text{CD}_3\text{CHD})_2\text{NH}$ and $\text{CD}_3\text{CHD}\text{NH}_2$, respectively. Thus, only little H/D exchange occurred (during the hydrogenation of CD_3CN of 0.83% the deuterons were found in products other than $\text{CD}_3\text{CH}_2\text{NH}_2$). With respect to the INS measurements, it can, thus, be stated that the signals obtained can be attributed to hydrogen atoms, which reacted with the CN triple bond and not to hydrogen, which exchanged with deuterons in the CD_3 group.

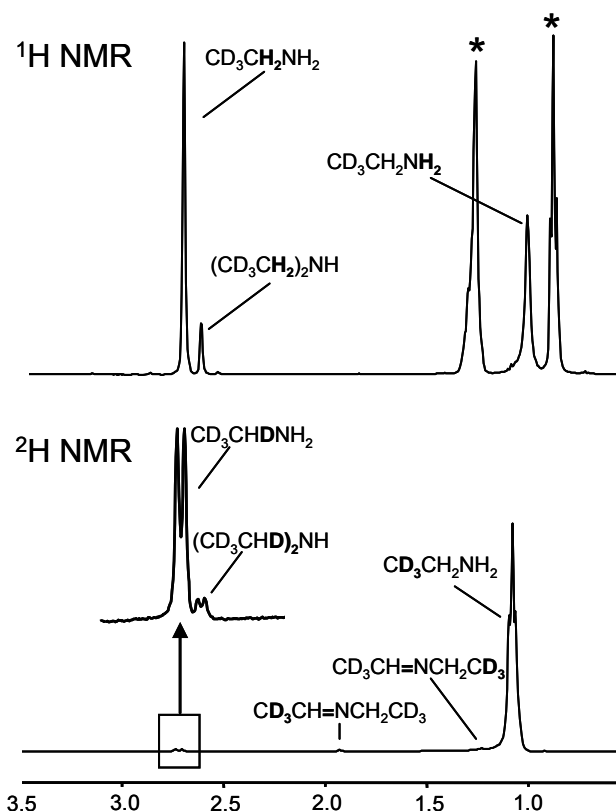


Fig. 5: NMR spectra of the product mixture of the hydrogenation of CD_3CN . * = Hexane.

4.3. Hydrogen adsorption on Raney-Co studied by INS

INS spectra of activated Raney-Co and of hydrogen adsorbed on Raney-Co were taken to evaluate contributions from the background. The results are presented in Fig. 6. The assignment of the hydrogen vibrations observed in the present work follow the detailed DFT analysis of the INS spectra of hydrogen adsorbed on Raney-Co reported previously¹³. In both spectra, scattering contributions of hydrogen gave rise to a broad peak between 600 and 1100 cm^{-1} centred at around 850 to 900 cm^{-1} . For the sample with activated Raney-Co, this suggests that some hydrogen could not be removed by the preparation procedure despite outgassing in high vacuum and at high temperature over several hours.

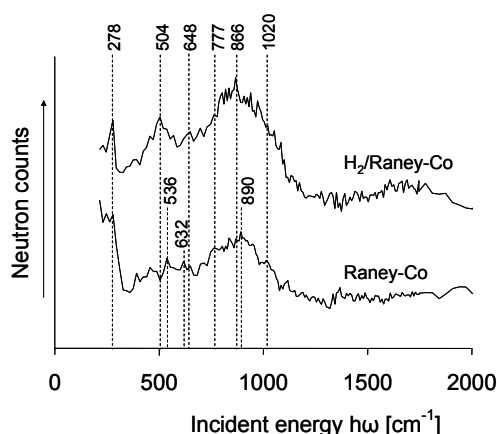


Fig. 6: INS spectrum of activated Raney-Co and INS spectrum of hydrogen adsorbed on Raney-Co after subtraction of the spectrum of Raney-Co. The amount of hydrogen admitted was calculated based on a stoichiometry of one hydrogen atom per surface metal atom as determined by H_2 chemisorption.

Tab. 3: Vibrational frequencies and assignment of hydrogen adsorbed on Raney-Co.

ν_{INS}^a	ν_{INS}^b	ν_{INS}^c	Coord. mode	Plane	Symmetry	Vibration ^{c,d,e}
278	278	250	η^4	101	D_{4h}	Co_4-H sym stretch
536	504	573	η^3	001	C_{3v}	Co_3-H antisym stretch
632	648	637	η^3	101	C_{3v}	Co_3-H antisym stretch
777	777	782	η^3	101	C_{3v}	Co_2-H asym stretch
890	866	894	η^3	001	C_{3v}	Co_2-H antisym stretch
1020	1020	1100	η^3	001	C_{3v}	Co_3-H sym stretch
-	>1600	1660	$f\sigma$	-	-	Co-H stretch

^aThis work (activated Raney-Co). ^bThis work (activated Raney-Co after addition of hydrogen). ^cRef ¹³.

^dRef ²². ^eRef ²⁰. ^fProbably hydrogen on some 1-fold sites. However, the DFT calculations of single bound hydrogen on 101 and 001 planes yields a peak at 1800 – 1860 cm^{-1} .

The band positions of residual hydrogen on activated Raney-Co and on Raney-Co loaded with extra hydrogen were in principle be the same. This suggests that strongly bound hydrogen was present, which withstood the rather severe activation conditions. The contributions in this region with strongly bound hydrogen can be attributed to hydrogen on η^3 sites (Tab. 3). Addition of hydrogen led to an increase in the scattering contributions over the whole range, especially in the range up to 1200 cm^{-1} . The distinct peak centred at 504 cm^{-1} results most likely from hydrogen adsorbed on η^3 sites with C_{3v} symmetry in the 001 plane. Upon addition of hydrogen small scattering contributions above 1500 cm^{-1} occurred probably due to some hydrogen adsorbed on σ sites. However, the signal was relatively small compared to multiply bound hydrogen.

4.4. Co-adsorption of CD_3CN and hydrogen on Raney-Co

To explore the structure and sorption properties of partially hydrogenated (intermediate-) species during the reaction between acetonitrile and hydrogen, a series of INS spectra of CD_3CN in presence of different amounts of hydrogen were measured. The INS spectra of CD_3CN , CD_3CN with 0.5, 1.5 and 2.0 equivalents of hydrogen and $CD_3CH_2NH_2$ adsorbed on activated Raney-Co are presented in Fig. 7.

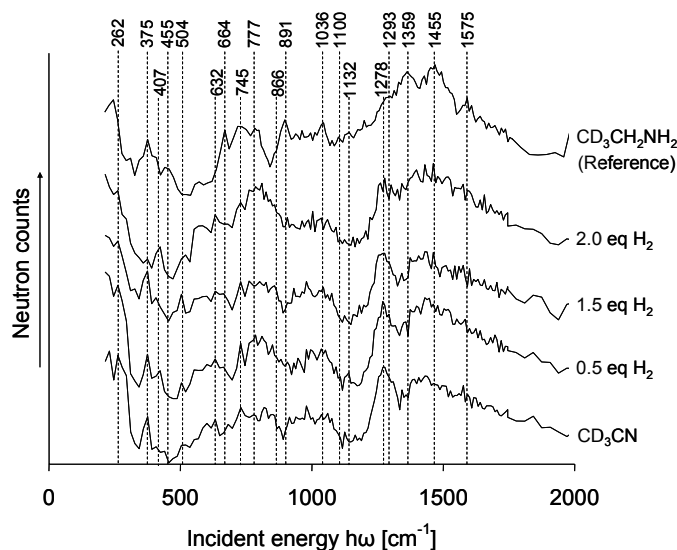


Fig. 7: INS spectra of different amounts of hydrogen co-adsorbed with CD_3CN (loading 0.18 molecules per surface metal atom) on activated Raney-Co. The amount of hydrogen was calculated based on a ratio of $\text{H}_2/\text{CD}_3\text{CN}$ of 0.5, 1.5 and 2.0, respectively. For comparison the spectra of CD_3CN and $\text{CD}_3\text{CH}_2\text{NH}_2$ adsorbed on activated Raney-Co are also given. The spectrum of activated Raney-Co has been subtracted from all the spectra shown.

In Table 4 experimental INS and IR frequencies for CH_3CN and CD_3CN from literature are compared to calculated vibrational modes from this work to verify the DFT data. From gas phase IR data and INS on solid CH_3CN it can be seen that slight deviations in the vibrational modes obtained with the two different techniques were obtained. INS data resulting from DFT calculations compared to gas phase IR data show a similar difference for CD_3CN . Thus, calculations are in good agreement with literature data reported by Friend et al.³⁰ The peaks with the highest intensity were assigned to the C-C-N bending mode at 354 cm^{-1} , the C-C stretching mode at 842 cm^{-1} and the CH_3 symmetric bending mode at 1138 cm^{-1} .

Tab. 4: Vibrational frequencies of CH_3CN and CD_3CN . Experimental data from literature together with vibrational frequencies of CD_3CN calculated by DFT.

CH_3CN		CD_3CN		Assignment
IR gas ^a	INS ^b	IR ^{c,#}	DFT ^d	
	75			Lattice mode
	120			Lattice mode
	160			Methyl torsion
361	396	347	354	CCN bend
920	928	902	842	CC stretch
1041	1056	(833)	(875)	$\text{CH}_3/(\text{CD}_3)$ rock
1389	1390	(1093)	(1138)	$\text{CH}_3/(\text{CD}_3)$ sym bend
1454	1453		(1067)	$\text{CH}_3/(\text{CD}_3)$ antisym def
2268		2291	2198	CN stretch
2954		(2110)	(2268)	$\text{CH}_3/(\text{CD}_3)$ sym stretch

^aRef³¹. ^bRef²¹. ^cRef³⁰. [#]Calculated from CH_3CN data by using deuteration shift ratios given in the reference. ^dThis work.

For assignment of the vibrational modes in the experimental INS data, the spectra obtained for species adsorbed on Raney-Co were compared to literature data of CH₃CN and CD₃CN (summarized in Table 5) and of ethylamine (see Table 6) adsorbed on different metals. No data for adsorbed CD₃CH₂NH₂ were available. However, gas phase IR data of non-deuterated ethylamine³²⁻³⁴ was previously compared to ethylamine adsorbed on Ni(111).³⁵ To conduct a similar comparison, DFT calculations were performed to obtain INS vibrational modes for pure CD₃CH₂NH₂. The experimental data together with DFT results are summarized in Table 6.

The spectrum of CD₃CN on Raney-Co exhibited a distinct peak at 375 cm⁻¹, a broad scattering region with strongly overlapping features between 600 and 1100 cm⁻¹, a distinct peak at 1278 cm⁻¹ and a broad peak starting at 1300 cm⁻¹ with a long tailing to 1800 cm⁻¹. The experimental results are compared to the calculated INS spectrum of CD₃CN in Fig. 9. It can be seen that there is little similarity of experiment and simulation. The fact that the rather distinct bands at 875 and 1067 cm⁻¹ were not observed in the experiment could be due to residual hydrogen masking the peaks. However, the intense bands at higher wave numbers (1278 – 1800 cm⁻¹) cannot be attributed to this effect, as was shown by the measurements of hydrogen adsorbed on Raney-Co. It had been reported that the vibrational modes of CD₃CN and CH₃CN can be strongly influenced upon adsorption on Pt (111) and Ni(111), respectively.^{30, 35, 36} In both cases one signal was not observed, while a new one appeared (shifted by up to 650 cm⁻¹) after adsorption. However, in general the spectra of the gas phase and the adsorbed state were similar and did not change in such a distinct manner as observed here.

Tab. 5: Selected literature data on the vibrations of CD₃CN and CH₃CN adsorbed on different metals.

CH ₃ CN			CD ₃ CN	
Raney-Ni ^a	Ni(111) ^b	Pt(111) ^c	Pt(111) ^c	Assignment
52				CH ₃ <i>torsion</i>
100				Hindered translations and motions
160				CH ₃ <i>torsion</i>
		280	265	Pt-MeCN <i>stretch sym</i>
		410	385	Pt-MeCN <i>stretch asym</i>
385, 392	360			CCN <i>bend</i>
520	520	605	580	CCN <i>bend</i>
	900 (sh)	950	930	CC <i>stretch</i>
1047, 1042	1020	1060	(850)	CH ₃ /(CD ₃) <i>rock</i>
1427, 1450	1400	1375	(1100)	CH ₃ /(CD ₃) <i>sym bend</i>
		1435		CH ₃ <i>deg bend</i>
	1680	1615	1625	CN <i>stretch</i>
	2910			CH ₃ <i>sym stretch</i>

^aRef²¹. ^bRef^{30, 35}. ^cRef³⁶.

Experimental INS data reported for CH₃CN adsorbed on Raney-Ni,²¹ which is expected to behave similar as Raney-Co, only showed little difference between CH₃CN in the gas phase and adsorbed on Raney-Ni. The results described above lead to the assumption that the observed INS spectrum was not due to CD₃CN coordinated to Raney-Co. It is rather likely that CD₃CN readily reacted with hydrogen not removed from the surface during the activation of Raney-Co resulting either in the formation of a nitrene or to the complete reaction to CD₃CH₂NH₂ or another intermediate.

In Fig. 7, the main peaks of $\text{CD}_3\text{CH}_2\text{NH}_2$ adsorbed on Raney-Co are marked and the respective wave number values are depicted. As shown in Table 6 INS data simulated with DFT for $\text{CD}_3\text{CH}_2\text{NH}_2$ are similar to the IR gas phase data for $\text{CH}_3\text{CH}_2\text{NH}_2$ as measured by Hamada et al.³² Hence, it was decided to perform assignment of most of the bands exhibited by $\text{CD}_3\text{CH}_2\text{NH}_2$ adsorbed on Raney-Co based on the literature available for $\text{CH}_3\text{CH}_2\text{NH}_2$ adsorbed on Ni(111). Additionally, it was decided to simulate the *trans* form of $\text{CD}_3\text{CH}_2\text{NH}_2$ because it was suggested in literature that compared to the *gauche* form this is the form, which more likely occurs on the surface.³⁵

Smaller differences in the vibrational modes of CH_2 , NH_2 , CCN , CC and CN are most likely due to the shift between INS and IR bands as previously described for CD_3CN , whereas the remarkable difference (shift from 2880 to 2176 cm^{-1}) in the CH_3 symmetric stretch band is attributed to the exchange of H by D in the methyl group. As shown in Table 6 most of the experimental INS band positions were similar to gas phase, DFT and literature data for adsorbed ethylamine and could, thus, be assigned accordingly. The shoulder peak at 407 cm^{-1} was also observed in the DFT results, but could not be assigned. An additional peak at 455 cm^{-1} may be due to cobalt-nitrogen vibrations as the value is comparable to nickel-nitrogen vibrations observed at 500 cm^{-1} for ethylamine on Ni(111)³⁵ and at 490 cm^{-1} for NH_3 on Ni(111).³⁷ DFT simulation exhibited bands at 499 and 596 cm^{-1} (not assigned), which were either overlapped or of too low intensity to find them in the experimental INS results. A band at 1293 cm^{-1} (shoulder) experimentally observed may be attributed to a shifted CH_2 twist, found at 1226 cm^{-1} in the simulated vibrations. In general, the relative peak intensity in the experiment is comparable to that from DFT calculations in the lower frequency region (up to $\sim 1200 \text{ cm}^{-1}$). At higher incident energy, the intensity of the bands is relatively high compared to the simulation.

The INS results of the adsorption of CD_3CN on Raney-Co in presence of increasing amounts of hydrogen showed similar features as for $\text{CD}_3\text{CH}_2\text{NH}_2$. However, differences were observed, which require further attention. Again, the data in Table 6 is consulted for band assignment. In order to distinguish co-adsorbed hydrogen from other surface species vibrations from Table 5 and Fig. 6 were also taken into account and marked in Fig. 7.

Upon adding hydrogen stepwise to CD_3CN , the scattering characteristics changed rendering spectra similar to the reference spectrum of $\text{CD}_3\text{CH}_2\text{NH}_2$. The spectra were similar to that for CD_3CN on Raney-Co, which again is an indication that CD_3CN was not the prevailing molecule in the sample. Additionally, it has to be considered that as shown in Fig. 6 hydrogen exhibits bands mainly in the region below 1200 cm^{-1} . Hence, the significant scattering contributions above this value can be attributed to partially hydrogenated or product molecules.

Tab. 6: Vibrational frequencies of CH₃CH₂NH₂ and CD₃CH₂NH₂ in the gas phase and adsorbed on different metals.

Gas phase			Ni(111) ^c	Raney-Co ^b	
gauche ^a	trans ^a	DFT ^b	HREELS	INS	Assignment
		297		245	NH ₂ rock
403		362		375	CCN bend
		664		664	CH ₂ rock
		755		745	CD ₃ bend
773	790	850	760	891	NH ₂ wag
892	882	975	880	1036	CC stretch
1016		955			NH ₂ twist
1016	1119	(1086)	1140	(1100)	CH ₃ /(CD ₃) rock
1086	1055	1122	1080	1132	CN stretch
1238	1350	1226		1293	CH ₂ twist
1378					CH ₃ sym def
1397		1387	>1360	1359	CH ₂ wag
1465			>1440		CH ₃ d def
1487		1508		1455	CH ₂ scission
1622		1673	1540	1575	NH ₂ scission
2880		(2176)	2960	-	CH ₃ /(CD ₃) sym stretch
		(2296)		-	CH ₃ /(CD ₃) asym stretch
2885		3040	2680	-	CH ₂ sym stretch

^aRef³²⁻³⁴, CH₃CH₂NH₂. ^bThis work, CD₃CH₂NH₂ in the *trans* form. ^cRef³⁵.

For the three samples with hydrogen and for the sample with CD₃CN a band at 262 cm⁻¹ was assigned to co-adsorbed hydrogen on η⁴ sites with D_{4h} symmetry. The CCN bending mode was located at 375 cm⁻¹. Again, a band at 407 cm⁻¹ was observed, which could not be clearly identified. The weak band at 504 cm⁻¹ was assigned to Co₃-H antisymmetric stretch on η³ coordination modes. In the region between 600 cm⁻¹ and 1200 cm⁻¹ features of the partially hydrogenated or product molecules were overlapping with scattering contributions of co-adsorbed hydrogen making unambiguous peak assignment difficult. However, it can be stated that upon increasing the amount of hydrogen a broad band centred at 777 cm⁻¹, which was previously assigned to Co₂-H asymmetric stretch η³ sites, increased. The band at 745 cm⁻¹ may be due to CD₃ bending modes. NH₂ wag and CC stretch modes found at 891 cm⁻¹ and 1036 cm⁻¹ for CD₃CH₂NH₂, respectively, were either relatively weak or overlapped by hydrogen vibration modes as no distinct peaks were found in that region. With exception of the hydrogen band at 777 cm⁻¹, no definitive trend in the intensity of the bands was obtained up to 1200 cm⁻¹. However, an interesting band was observed at 1278 cm⁻¹ exhibiting relatively high intensity for CD₃CN only. Compared to the broad signal above 1300 cm⁻¹ the relative intensity of this band decreased with increasing amount of hydrogen. In the case of CD₃CH₂NH₂ a shoulder at 1293 cm⁻¹ was attributed to a CH₂ twisting mode. It will be considered in the discussion section, if this mode is also responsible for the relatively strong signal in the case of co-adsorption of CD₃CN and hydrogen

A broad band between 1300 and 1800 cm⁻¹ was found for all samples with CD₃CN and CD₃CN plus hydrogen being similar to the pattern observed for CD₃CH₂NH₂. Compared to the band at 1278 cm⁻¹ the relative intensity of the band increased with increasing amount of hydrogen. This is an indication that an intermediate species was

converted upon adding hydrogen resulting in an increasing amount of $\text{CD}_3\text{CH}_2\text{NH}_2$. However, the single peaks as found for $\text{CD}_3\text{CH}_2\text{NH}_2$ at 1359, 1455 and 1575 cm^{-1} were not as well resolved suggesting that other molecules were present which exhibited a different scattering behaviour. Thus, the broad band would be a result of overlapping signals from $\text{CD}_3\text{CH}_2\text{NH}_2$ and intermediate species.

4.5. Role of hydrogen sorption strength

For Raney-Ni the presence of different sites strongly and weakly adsorbing hydrogen has been reported.²² The presence of strongly and weakly bound hydrogen was also indicated by H_2 chemisorption and INS experimental results for hydrogen adsorbed on Raney-Co. The two techniques cannot be directly compared but provide complementary results. INS measurements of activated Raney-Co showed that strongly bound hydrogen could not be removed from the surface by the activation procedure. The sample for H_2 chemisorption measurements underwent the same pre-treatment before adding hydrogen stepwise. Thus, hydrogen residing on the catalyst surface after pre-treatment could not be quantified. However, it was found that hydrogen was partly chemisorbed and partly physisorbed suggesting that two different sorption sites are present on activated Raney-Co. Hence, taking into account hydrogen not removed during the activation procedure three different levels of adsorption prevail (strongly chemisorbed, chemisorbed and physisorbed hydrogen).

In the INS experiments, the three levels could not be distinguished, but sorption sites for hydrogen were identified. Taking into account the experiments with varying amounts of hydrogen co-adsorbed with CD_3CN one may get insight into the reactivity of hydrogen adsorbed on those different sites. Especially in the sample with 2.0 equivalents of hydrogen it was observed that differences occur between Raney-Co and hydrogen co-adsorbed with CD_3CN assuming that reaction took place, but not all of the hydrogen added reacted. As it cannot be excluded that scattering contributions of intermediate species or $\text{CD}_3\text{CH}_2\text{NH}_2$ were overlapping with bands of non-reacted hydrogen the discussion will be restricted to bands, which can be attributed to hydrogen mainly. Upon increasing the amount of hydrogen scattering contributions assigned to hydrogen increased relatively strongly in the region around 632 and 777 cm^{-1} (hydrogen on η^3 sites with C_{3v} symmetry on the 101 plane). Whereas scattering contributions at 504 , 866 and 1020 cm^{-1} (all of them corresponding to various vibrational modes of hydrogen on η^3 sites with C_{3v} symmetry on the 001 plane) increased less. Therefore, it is suggested that hydrogen adsorbed on the latter sites preferably reacted with CD_3CN . In agreement with literature,²² it is concluded that hydrogen on latter sites is weakly chemisorbed hydrogen, as this kind of hydrogen is more reactive.

4.6. Intermediate species in the co-adsorption of CD_3CN and hydrogen on Raney-Co

Results of the INS experiment with CD_3CN as sole adsorbate did not show significant agreement with literature data of gas phase and adsorbed CD_3CN .³⁶ Also the INS spectrum of CD_3CN calculated with (shown in Fig. 9 for comparison) was quite different from experimental data especially at higher incident energy (above 1200 cm^{-1}). Thus, it was concluded that a species other than CD_3CN , which was formed by reac-

tion with residual hydrogen prevailed on the surface. The assumption that a reaction took place is supported by TG/DSC results showing that on one type of sites strong adsorption of CD_3CN occurred, which leads to strong activation and hence high reactivity of CD_3CN .

Based on the assumption that a reaction took place, the question arises, which species are formed. The most obvious explanation would be that CD_3CN was completely converted to $\text{CD}_3\text{CH}_2\text{NH}_2$. As described above there are, in deed, some similarities with the spectrum of $\text{CD}_3\text{CH}_2\text{NH}_2$, but it has also been shown that remarkable differences appeared. Especially the relatively strong band at 1278 cm^{-1} was much weaker (and slightly shifted to 1293 cm^{-1}) for $\text{CD}_3\text{CH}_2\text{NH}_2$ compared to the samples with CD_3CN co-adsorbed with hydrogen. Hence, it is suggested that a mixture of intermediate species, of which the most characteristic feature is the band at 1278 cm^{-1} and $\text{CD}_3\text{CH}_2\text{NH}_2$ co-exist on the surface. When increasing the hydrogen pressure, the peak area decreased relative to the band regions, which are more characteristic for $\text{CD}_3\text{CH}_2\text{NH}_2$ (above 1300 cm^{-1}). This observation suggests that by increasing the hydrogen pressure the equilibrium was shifted to fully hydrogenated product. Partially hydrogenated intermediate species co-exist, however, only on the surface if they are energetically comparable to adsorbed $\text{CD}_3\text{CH}_2\text{NH}_2$. In this respect, it has been shown in a molecular modelling study of amine dehydrogenation over Ni(111) that the partly dehydrogenated intermediate acimidoyl ($\text{CH}_3\text{-C}^*\text{=NH}$, where * symbolizes coordination to a metal atom) was energetically lower than adsorbed ethylamine.³⁸

Before discussing sorption structures of possible intermediates, the adsorption mode of $\text{CD}_3\text{CH}_2\text{NH}_2$ will be examined. Based on observations in literature^{35, 37} it is suggested that it is adsorbed molecularly through its nitrogen lone pair electrons. The existence of a cobalt-nitrogen stretching mode supports this assumption. For the experimental spectrum of $\text{CD}_3\text{CH}_2\text{NH}_2$ the band at 1293 cm^{-1} was assigned to CH_2 twisting. For the same mode DFT calculations predict a band at 1226 cm^{-1} . Conversely, CH_2 wagging was shifted to a lower frequency upon adsorption on Raney-Co. In literature it was suggested that interaction of hydrogen with Ni(111) surface weakened the CH bond.^{35, 39} However, with the results obtained in this study this cannot be stated unambiguously.

Above it has been established that intermediate species are formed during co-adsorption of CD_3CN and hydrogen. The structure of this intermediate requires elucidation. In principle several surface structures are possible after reaction of CD_3CN with 2 atoms of hydrogen. In Fig. 8, three such surface structures as proposed in literature are summarized. Here, it will be discussed, which of the intermediates is most likely according to the INS experiments.

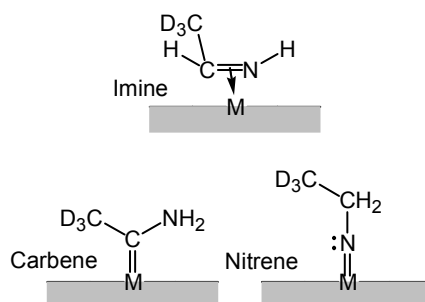


Fig. 8: Surface structures after reaction of CD_3CN with 2 hydrogen atoms based on suggestions found in the literature.^{8,40}

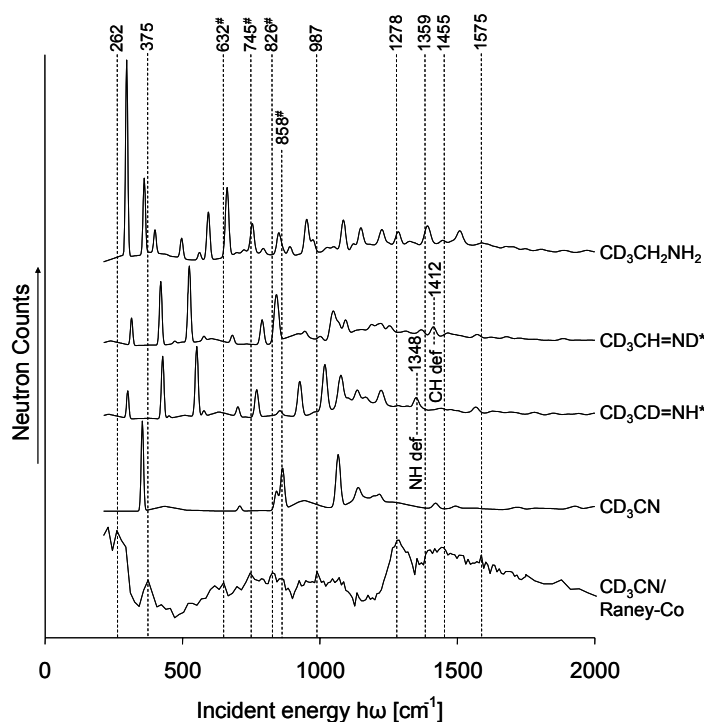


Fig. 9: Experimental INS spectrum of CD_3CN adsorbed on activated Raney-Co compared to calculated gas phase INS spectra of reactant, possible intermediate and product species. #Region in which significant hydrogen contributions were observed for activated Raney-Co. *Calculated as a model for surface imine species. Exchanging H and D was performed to differentiate between CH and NH vibrational modes.

In order to investigate if imine-like species were formed INS data for pure imine were calculated by means of DFT and compared to experimental results (presented in Fig. 9). As H atoms exhibit much higher intensity they were selectively exchanged by D atoms in the CN double bond to differentiate between contributions of CH and NH vibrational modes. The experimental spectrum for CD_3CN on Raney-Co is shown as comparison, as the band at 1278 cm^{-1} , which is assumed to be related with the intermediate species, is most intense. The high intensity suggests that H atoms must be involved in this vibrational mode. For comparison, the simulated spectra of CD_3CN and $CD_3CH_2NH_2$ are shown. Distinct bands of the experimental spectrum are marked to evaluate the agreement with calculated spectra. However, it can be seen that the

experimental data is somewhat noisy with not always clearly resolved peaks and may be overlapped by hydrogen in the region between 632 and 858 cm^{-1} . Additionally, the relative band intensity in the experimentally determined spectrum for $\text{CD}_3\text{CH}_2\text{NH}_2$ is quite different from the simulated spectrum, which might be an indication for very strong interaction with the surface. In none of the simulated spectra, such a distinct peak at 1278 cm^{-1} is predicted. In the simulated imine spectra, the vibrations involving hydrogen closest to this strong band are depicted. The NH deformation of $\text{CD}_3\text{CD}=\text{NH}$ exhibited a low intensity band at 1348 cm^{-1} . CH deformation of $\text{CD}_3\text{CH}=\text{ND}$ resulted in a band with even lower intensity at 1412 cm^{-1} . π -Coordination of the imine to the surface (see Fig. 8) may result in a blue shift leading to the experimentally observed bands at 1278 cm^{-1} and 1387 cm^{-1} , respectively. However, due to the agreement of the strong band at 1278 cm^{-1} with the experimentally obtained band at 1293 cm^{-1} for CH_2 twisting modes of $\text{CD}_3\text{CH}_2\text{NH}_2$ it is assumed that it appears more likely that this mode is responsible for the strong band. Thus, no evidence for the existence of an imine-like intermediate was found.

Of the two species carbene and nitrene (shown in Fig. 8), only nitrene can have CH_2 vibrational modes. Hence, only this compound may exhibit the band at 1278 cm^{-1} due to CH_2 twisting. In Fig. 7, the NH_2 wagging mode resulted in a relatively well-resolved band at 891 cm^{-1} for $\text{CD}_3\text{CH}_2\text{NH}_2$. No such distinct band was observed for the other spectra. It is assumed that hydrogen did not overlap the peak, which is appropriate, as the amount of hydrogen in the sample with CD_3CN and $\text{CD}_3\text{CH}_2\text{NH}_2$ only, was the same due to the same activation procedure. Hence, it is concluded that NH_2 groups were only of low concentration in the intermediate surface species suggesting that nitrene species were the most abundant intermediates. However, the question arises, why CH_2 twisting modes should be more intense relative to the CH_2 wagging and deformation modes with bands at 1359 cm^{-1} and 1455 cm^{-1} , respectively, in nitrene than in $\text{CD}_3\text{CH}_2\text{NH}_2$. This can tentatively be explained by assuming different adsorption modes of the respective molecules. As mentioned above $\text{CD}_3\text{CH}_2\text{NH}_2$ adsorbs most likely *via* its nitrogen lone electron pair resulting in an N-M σ -bond, whereas nitrene results in a N-M double bond. It is suggested that the CH_2 twisting mode leads to a torsional movement of the NM bond resulting in little change in the orbital overlap of nitrogen and the metal. Hence, the difference between the two bonding modes might be smaller than with CH_2 wagging. This movement causes a stretch of the C-M bond, in which the change of the orbital overlap is considerably higher. Consequently, the CH_2 wagging may have higher intensity with $\text{CD}_3\text{CH}_2\text{NH}_2$, as the overlap can take place more easily in a σ -bond.

Transition metal complexes can be used for comparison to help in the interpretation of the actual catalysis mechanism.⁸ Therefore, a search of the Cambridge Crystallographic Database was performed and several stable nitrene-like intermediates were found.^{41, 42} One of the complexes is exemplarily shown in Fig. 10, supporting the assumption that similar nitrene species might also prevail in the hydrogenation over Raney-Co catalysts. In fact, they have also been reported in surface studies on a Ni/C catalyst⁴³ and suggested to be the most stable intermediates in the hydrogenation of acetonitrile over Ni surfaces based on DFT results.³

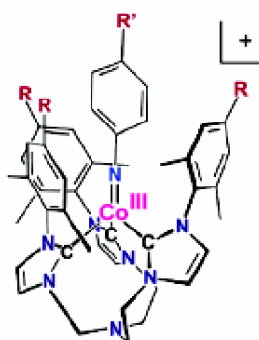


Fig. 10: Organometallic complex with nitrene functionality.⁴²

5. Conclusions

Experimental and calculated INS spectra were combined with spectroscopic data from literature to examine partly hydrogenated surface species in the co-adsorption of CD_3CN and H_2 on Raney-Co. As INS is very sensitive to H atoms, CD_3CN was used as a probe molecule to keep scattering contributions stemming from the methyl group low. Preparatory experiments showed that very little H/D exchange occurred during hydrogenation of CD_3CN , which resulted in high selectivity (90%) to $\text{CD}_3\text{CH}_2\text{NH}_2$. In TG/DSC measurements, two different types of sites for the adsorption of CD_3CN were found. One type shows a particularly strong interaction with CD_3CN . Combination with H_2 chemisorption results showed that at the maximum sorption capacity for CD_3CN $\sim 30\%$ of the cobalt surface atoms were occupied.

The combination of INS and H_2 chemisorption results confirmed that under the conditions applied three levels of hydrogen adsorption were present (strong chemisorption, chemisorption and physisorption). Additionally, it was suggested that hydrogen adsorbed on η^3 sites with C_{3v} symmetry was less strongly bound than hydrogen adsorbed on other sites and, thus, most reactive. Comparison of simulated and measured INS results confirmed that the sorbates strongly interacted with the adsorption sites. A band at 1278 cm^{-1} , which was relatively strong in the samples with co-adsorbed CD_3CN and H_2 and decreased in intensity with increasing amount of H_2 , was tentatively assigned to the CH_2 twisting mode. The relative decrease of this band compared to CH_2 wagging led to the assumption that a nitrene-like compound was the most abundant intermediate species on the surface.

6. Acknowledgement

The authors thank the Institut Laue-Langevin for kindly granting measuring time at the IN1-BeF spectrometer to record the INS spectra. In particular, Dr. Alexander Ivanov and Pierre Palleau are thanked for their assistance during the INS experiments. W. R. Grace & Co is thanked for the donation of the Raney-Co 2700 sample. Experimental support of Xaver Hecht and Manuel Stratmann is acknowledged. Klaus Ruhland and Ceta Krutsch from the Chair of Inorganic Chemistry are acknowledged for performing the NMR measurements.

7. References

1. Weissermel, K., Arpe, H.J., *Industrial Organic Chemistry*. 3. ed. 1997, Weinheim: Wiley-VCH.
2. von Braun, J., Blessing, G., Zobel, F., *Catalytic hydration under pressure in the presence of nickel salts, VI. Nitriles*. Berichte der Deutschen Chemischen Gesellschaft, 1923. 56. p. 1988-2001.
3. Bigot, B., Delbecq, F., Milet, A. and Peuch, V.H., Nitriles and hydrogen on a nickel catalyst: Theoretical evidence of a process competing with the total hydrogenation reaction. *J. Catal.*, 1996. 159(2). p. 383-393.
4. Bigot, B., Delbecq, F., Peuch, V.H., Adsorption Modes of Acetonitrile on Ni(111), Ni(100), and Ni(110) - A Semiempirical Theoretical-Study. *Langmuir*, 1995. 11(10). p. 3828-3844.
5. Huang, Y.Y., Sachtler, W.M.H., On the mechanism of catalytic hydrogenation of nitriles to amines over supported metal catalysts. *Appl. Catal. A-Gen.*, 1999. 182(2). p. 365-378.
6. Huang, Y.Y., Sachtler, W.M.H., *Catalytic hydrogenation of nitriles over supported mono- and bimetallic catalysts*. *J. Catal.*, 1999. 188(1). p. 215-225.
7. Coq, B., Tichit, D., Ribet, S., Co/Ni/Mg/Al layered double hydroxides as precursors of catalysts for the hydrogenation of nitriles: Hydrogenation of acetonitrile. *J. Catal.*, 2000. 189(1). p. 117-128.
8. DeBellefon, C., Fouilloux, P., Homogeneous And Heterogeneous Hydrogenation Of Nitriles In A Liquid-Phase - Chemical, Mechanistic, And Catalytic Aspects. *Catal. Rev.-Sci. Eng.*, 1994. 36(3). p. 459-506.
9. Huang, Y.Y., Sachtler, W.M.H., Intermolecular hydrogen transfer in nitrile hydrogenation over transition metal catalysts. *J. Catal.*, 2000. 190(1). p. 69-74.
10. Huang, Y.-Y., Sachtler, W.M.H., *Catalytic hydrogenation of nitriles to prim., sec. and tert. amines over supported mono- and bimetallic catalysts*. *Studies in Surface Science and Catalysis*, 2000. 130A(International Congress on Catalysis, 2000, Pt. A). p. 527-532.
11. Wainwright, M.S., in *Preparation of Solid Catalysts*, G. Ertl, H. Knözinger, and J. Weitkamp, Editors. 1999, Wiley-VCH: Weinheim. p. 28-43.
12. Volf, J., Pasek, J., *Hydrogenation of nitriles*. *Studies in Surface Science and Catalysis*, 1986. 27(Catal. Hydrogenation). p. 105-144.
13. Chojecki, A., Jobic, H., Jentys, A., Muller, T.E. and Lercher, J.A., *Inelastic neutron scattering of hydrogen and butyronitrile adsorbed on Raney-Co catalysts*. *Catal. Lett.*, 2004. 97(3-4). p. 155-162.
14. Chojecki, A., *Selective Hydrogenation of Butyronitrile over Raney-Metals*. (2004), TU München Dissertation. 116 pp.
15. Scharringer, P., Muller, T.E., Kaltner, W. and Lercher, J.A., *In situ measurement of dissolved hydrogen during the liquid-phase hydrogenation of dinitriles-method and case study*. *Industrial & Engineering Chemistry Research*, 2005. 44(25). p. 9770-9775.
16. Schenkel, R., Jentys, A., Parker, S.F. and Lercher, J.A., *INS and IR and NMR spectroscopic study of C-1-C-4 alcohols adsorbed on alkali metal-exchanged zeolite X*. *Journal Of Physical Chemistry B*, 2004. 108(39). p. 15013-15026.
17. Parker, S.F., Taylor, J.W., Albers, P., Lopez, M., Sextl, G., Lennon, D., McInroy, A.R. and Sutherland, I.W., *Inelastic neutron scattering studies of hydrogen on fuel cell catalysts*. *Vibrational Spectroscopy*, 2004. 35(1-2). p. 179-182.
18. Vasudevan, S., Thomas, J.M., Wright, C.J. and Sampson, C., *Inelastic Neutron-Scattering Studies Of Hydrogen Uptake By A Model Hydrodesulfurization Catalyst At High-Pressure*. *J. Chem. Soc.-Chem. Commun.*, 1982(7). p. 418-419.

19. Schenkel, R., Jentys, A., Parker, S.F. and Lercher, J.A., *Investigation of the adsorption of methanol on alkali metal cation exchanged zeolite X by inelastic neutron scattering*. Journal Of Physical Chemistry B, 2004. 108(23). p. 7902-7910.
20. Jobic, H., Renouprez, A., *Inelastic Neutron-Scattering Spectroscopy Of Hydrogen Adsorbed On Raney-Nickel*. Journal Of The Chemical Society-Faraday Transactions I, 1984. 80. p. 1991-1997.
21. Hochard, F., Jobic, H., Clugnet, G., Renouprez, A. and Tomkinson, J., *Inelastic Neutron-Scattering Study Of Acetonitrile Adsorbed On Raney-Nickel*. Catal. Lett., 1993. 21(3-4). p. 381-389.
22. Hochard, F., Jobic, H., Massardier, J. and Renouprez, A.J., *Gas-Phase Hydrogenation Of Acetonitrile On Raney-Nickel Catalysts - Reactive Hydrogen*. J. Mol. Catal. A-Chem., 1995. 95(2). p. 165-172.
23. <http://www.ill.fr/YellowBook/INI>.
24. Frisch, M.J.T., G. W.; Schlegel, H. B.; Scuseria, G. E.; Robb, M. A.; Cheeseman, J.R.Z., V. G.; Montgomery, J. A., Jr., Stratmann, R.E.B., J. C.; Dapprich, S.; Millam, J. M.; Daniels, A., D.; Kudin, K.N.S., M. C.; Farkas, O.; Tomasi, J.; Barone, V.; Cossi, M.; Cammi, R.M., B.; Pomelli, C.; Adamo, C.; Clifford, S.; Ochterski, J.P., G. A.; Ayala, P. Y.; Cui, Q.; Morokuma, K.; Malick, D. K.; Rabuck, A.D.R., K.; Foresman, J. B.; Cioslowski, J., Ortiz, J.V.B., A. G.; Stefanov, B. B.; Liu, G.; Liashenko, A.; Piskorz, P.; Komaromi, I.G., R.; Martin, R. L.; Fox, D. J.; Keith, T.; Al-Laham, M.A.P., C. Y.; Nanayakkara, A.; Challacombe, M.; Gill, P., M. W.; Johnson, B.C., W.; Wong, M. W.; Andres, J. L.; Gonzalez, C.; and Head-Gordon, M.R., E. S.; Pople, J. A., *GAUSSIAN 98*. (1998), Gaussian, Inc.: Pittsburgh, PA.
25. Champion, D., Tomkinson, J., Kearley, G., *a-CLIMAX: a new INS analysis tool*. Applied Physics A-Materials Science & Processing, 2002. 74. p. S1302-S1304.
26. Ramirez-Cuesta, A.J., *aCLIMAX 4.0.1*, The new version of the software for analyzing and interpreting INS spectra. Computer Physics Communications, 2004. 157(3). p. 226-238.
27. Jentys, A., Mukti, R.R., Tanaka, H. and Lercher, J.A., *Energetic and entropic contributions controlling the sorption of benzene in zeolites*. Microporous And Mesoporous Materials, 2006. 90(1-3). p. 284-292.
28. Hesse, M., Meier, H., Zeeh, B., *Spektroskopische Methoden in der organischen Chemie*. 3 ed. 1987, Stuttgart: Georg Thieme Verlag. 318.
29. Pretsch, E., Clerc, T., Seibl, J. and Wilhelm, S., *Tabellen zur Strukturaufklärung organischer Verbindungen mit spektroskopischen Methoden*. 3 ed. Anleitungen für die chemische Laboratoriumspraxis, ed. W. Fresenius, et al. Vol. 15. 1986, Berlin: Springer-Verlag.
30. Friend, C.M., Muettterties, E.L., Gland, J.L., *Vibrational Studies Of Ch₃cn And Ch₃nc Adsorbed On Ni(111) And Ni(111)-C Surfaces*. Journal Of Physical Chemistry, 1981. 85(22). p. 3256-3262.
31. Davies, J.E.D., *Raman Spectra Of Guest Molecules Formic Acid, Methanol, And Acetonitrile In Beta-Quinol Clathrates*. Journal Of Molecular Structure, 1971. 9(4). p. 483-&.
32. Hamada, Y., Hashiguchi, K., Hirakawa, A.Y., Tsuboi, M., Nakata, M., Tasumi, M., Kato, S. and Morokuma, K., *Vibrational Analysis Of Ethylamines - Trans And Gauche Forms*. Journal Of Molecular Spectroscopy, 1983. 102(1). p. 123-147.
33. Wolff, H., Ludwig, H., *Raman Spectra Of Gaseous Ch₃nd₂, C₂h₅nd₂, And C₃h₇nd₂ - Raman And Infrared-Spectra Of Gaseous Ch₃nhd*. Journal Of Chemical Physics, 1972. 56(11). p. 5278-&.
34. Wolff, H., Ludwig, H., *Raman And Ur Spectra Of Crystallized Primary Aliphatic Amines And Their N-Deutero Derivatives*. Berichte Der Bunsen-Gesellschaft Fur Physikalische Chemie, 1967. 71(8). p. 911-&.

35. Gardin, D.E., Somorjai, G.A., *Vibrational-Spectra And Thermal-Decomposition Of Methylamine And Ethylamine On Ni(111)*. Journal Of Physical Chemistry, 1992. 96(23). p. 9424-9431.
36. Sexton, B.A., Avery, N.R., Coordination Of Acetonitrile (Ch₃cn) To Platinum (111) - Evidence For An Eta-2 (C,N) Species. Surface Science, 1983. 129(1). p. 21-36.
37. Gland, J.L., Fisher, G.B., Mitchell, G.E., *Vibrational Characterization Of Adsorbed Nh On The Ni(111) Surface*. Chemical Physics Letters, 1985. 119(1). p. 89-92.
38. Ditlevsen, P.D., Gardin, D.E., Vanhove, M.A.andSomorjai, G.A., *Molecular Modeling Of Amine Dehydrogenation On Ni(111)*. Langmuir, 1993. 9(6). p. 1500-1503.
39. Raval, R., Chesters, M.A., The Nature Of The C-H. Metal Interaction In Adsorbed Cyclohexane And Its Role In Reactivity. Surface Science, 1989. 219(1-2). p. L505-L514.
40. Chojecki, A., Veprek-Heijman, M., Müller, T.E., Schäringer, P., Veprek, S.andLercher, J.A., *Tailoring Raney-catalysts for the selective hydrogenation of butyronitrile to n-butylamine*. J. Catal., 2007. 245. p. 237-248.
41. Shay, D.T., Yap, G.P.A., Zakharov, L.N., Rheingold, A.L.andTheopold, K.H., *Intramolecular C-H activation by an open-shell cobalt(N) imido complex*. Angew. Chem.-Int. Edit., 2005. 44(10). p. 1508-1510.
42. Hu, X., Meyer, K., Terminal cobalt(III) imido complexes supported by tris(carbene) ligands: Imido insertion into the cobalt-carbene bond. Journal Of The American Chemical Society, 2004. 126(50). p. 16322-16323.
43. Bock, H., Breuer, O., *Surface-Reactions.8. Decarbonylation On Carbon-Supported Nickel-Catalysts*. Angew. Chem.-Int. Edit. Engl., 1987. 26(5). p. 461-462.